

Neural Response Selectivity to Natural Sounds in the Bat Midbrain

Angeles Salles,^{a*} Sangwook Park,^b Harshavardhan Sundar,^b Silvio Macías,^a Mounya Elhilali^b and Cynthia F. Moss^a

^a Department of Psychological and Brain Sciences, Johns Hopkins University, United States

^b Department of Electrical and Computer Engineering, Johns Hopkins University, United States

Abstract—Little is known about the neural mechanisms that mediate differential action–selection responses to communication and echolocation calls in bats. For example, in the big brown bat, frequency modulated (FM) food-claiming communication calls closely resemble FM echolocation calls, which guide social and orienting behaviors, respectively. Using advanced signal processing methods, we identified fine differences in temporal structure of these natural sounds that appear key to auditory discrimination and behavioral decisions. We recorded extracellular potentials from single neurons in the midbrain inferior colliculus (IC) of passively listening animals, and compared responses to playbacks of acoustic signals used by bats for social communication and echolocation. We combined information obtained from spike number and spike triggered averages (STA) to reveal a robust classification of neuron selectivity for communication or echolocation calls. These data highlight the importance of temporal acoustic structure for differentiating echolocation and food-claiming social calls and point to general mechanisms of natural sound processing across species. © 2019 IBRO. Published by Elsevier Ltd. All rights reserved.

Key words: big brown bats, echolocation, social communication sounds, inferior colliculus.

INTRODUCTION

Echolocating bats produce sonar signals and process auditory information carried by returning echoes to represent the spatial layout of objects in their surroundings (Griffin, 1958; Popper and Fay, 1995; Thomas et al., 2003). Acoustic information that the bat obtains from its surroundings comes not only from self-generated echo returns, but also from echolocation and social communication sounds produced by neighboring conspecifics. As such, the mix of echolocation and social communication sounds creates a cocktail party-like environment (Cherry, 1953; Lewicki et al., 2014), in which bats operate. Most bat communication and echolocation calls contain overlapping acoustic features. Yet, animals must distinguish between these classes of sounds in order to successfully extract behaviorally relevant information. The neural basis for discriminating these functionally distinct acoustic signals is the focus of our study.

The echolocating bat's acoustic scene is complex and dynamic. Many insectivorous species use frequency modulated (FM) sonar signals, and they adapt the duration and rate of calls in response to 3D spatial

information computed from returning echoes. Such dynamic changes in sonar signals allow the bat to select the acoustic features of echoes that guide it through the search, tracking and interception stages of insect capture (reviewed in Schnitzler and Kalko (2001)).

As bats forage, they also produce a rich repertoire of social calls. One social call of the big brown bat (*Eptesicus fuscus*) the *Frequency Modulated Bout* (FMB), is postulated to serve a food-claiming function, as this signal is produced only by male bats of this species under competitive foraging conditions, and the individual emitting the FMB is typically successful in taking the insect prey (Wright et al., 2013). The FMB is comprised of a sequence of three to four calls, with call intervals of 21–28 ms. While the echolocation and FMBs both sweep from high to low sound frequencies, with spectral energy between 25 and 100 kHz, we hypothesize that fine differences in the temporal structure of these signal categories drive separable auditory responses in neuronal populations, which supports behavioral discrimination of FMB social and FM echolocation calls.

A central hub in auditory processing and the focus of our study is the inferior colliculus (IC), a midbrain structure that receives both ascending input from brainstem nuclei and descending input from auditory cortex. Broadly important to comparative studies of brain and behavior, the IC has been implicated in auditory coding in a wide range of species (Sayegh et al., 2011). Furthermore, in some bat species, IC neu-

*Corresponding author. Address: Department of Psychological and Brain Sciences, Johns Hopkins University, Ames Building, 3400 N. Charles Street, Baltimore, MD 21218, United States.

E-mail address: angiesalles@jhu.edu (A. Salles).

Abbreviations: FM, frequency modulated; FMB, *Frequency Modulated Bout*; IC, inferior colliculus; STA, spike triggered averages.

rons show selectivity to species-specific communication calls (Mexican free-tailed bat, *Tadarida brasiliensis mexicana*, (Pollak, 2011); mustached bat, *Pteronotus parnellii*, (Portfors, 2004)). Artificial FM sweeps matched in bandwidth and sweep rate but differing in the direction of the sweep (upward or downward), evoke distinct neural responses in populations of spectral motion selective neurons (Andoni and Pollak, 2011). In the mustached bat, pure tones do not evoke responses in communication call-selective neurons; however, particular combinations of tones evoke responses similar to those evoked by natural calls (Portfors, 2004). Taken together, these findings suggest that selectivity to communication sounds is driven by a combination of spectral and temporal acoustic parameters.

Neural selectivity at a population level to functionally-defined species-specific social calls has yet to be systematically studied in echolocating bats. Here, we bridge this gap by quantifying neural response selectivity in the auditory midbrain IC of the big brown bat to functionally characterized social and echolocation calls used by this species. Specifically, our study investigates neural selectivity to food-claiming FMB social and FM echolocation calls. We hypothesize that separate populations of neurons in the midbrain IC of the big brown bat show differentially selective responses to social and echolocation calls, which could mediate the behavioral discrimination of sounds that serve different functions.

EXPERIMENTAL PROCEDURES

Animals

Five wild big brown bats (*E. fuscus*) were used for the experiments, two males and three females. Bats were collected in the state of Maryland under the collecting permit number 55440, issued by the Maryland Department of Natural Resources. All experimental protocols and neurophysiological recording procedures were approved by The Johns Hopkins University Institutional Animal Care and Use Committee.

Acoustic stimuli

Broadcasts of communication and echolocation calls were presented to awake, passively listening animals while taking extracellular recordings from the IC with a 16-channel silicon probe. Six exemplars of FMB (communication calls) were selected from archived data previously recorded in the laboratory from bats foraging in a competitive environment (Chiu et al., 2008; Wright et al., 2014). FMB's comprise sets of 3–4 frequency modulated sweeps (characterized in (Wright et al., 2013)) with an inter-call interval ranging from 22.6 ms to 28.2 ms. Each call had an average duration of 6.3 ms, and the frequency bandwidth spans 22–110 kHz over two harmonics with high signal to noise ratio. All stimuli were broadcast at 70 dB SPL at the position of the bat. Six echolocation sequences were built using natural echolocation calls and the inter-call interval was fixed to match the timing of each call in the FMB's. Echolocation calls were

selected from the same data set as the communication calls, which were approximately matched in duration and bandwidth to the FMB elements (5.9 ms \pm 0.6 ms and 27–110 kHz). Isolated single elements of FMB and echolocation calls were also presented to the passively listening bat (Fig. 1A). To compare the signal profiles of FMB and echolocation calls, two types of analyses were performed; First, the time–frequency spectrogram of each call was visually inspected by calculating frequency modulation (FM) slopes at the points that were manually marked at 0.6 ms intervals (Fig. 1A). The coordinates of these points were then used to calculate the FM slope for each interval defined $\frac{\Delta f}{\Delta t}$. An array of such slopes was pooled for the first and second harmonic of each call and an unpaired t-test was performed comparing the distribution of slopes from each harmonic component of FMB and echolocation calls. Second, each time–frequency spectrogram was further analyzed in the modulation domain through an array of two-dimensional Gabor filters, following classic techniques used for modulation analysis of complex sounds (Chi et al., 2005). The Gabor filters are tuned over the rate 0.33–3.25 cycle/octave along the scale (spectral modulation) axis and 200–650 Hz along the rate (temporal modulation) axis. Note that the positive and negative rate values mean the downward and upward variation, respectively.

To build frequency tuning curves for neurons recorded in the IC, pure tones of 5 ms duration (with 0.5 ms ramping rise and fall) ranging frequencies between 20 and 90 kHz (5 kHz steps) were broadcast at different sound pressure levels ranging from 20 to 70 SPL (10 dB steps), corrected for the loudspeaker frequency response. Each pure tone at each SPL was randomly presented 15 times at a 300 ms inter-stimulus interval.

All stimuli were generated at a sampling rate of 250 kHz using a National Instruments card (PXIe 6358) and transmitted to an audio amplifier (Krohn-Hite 7500). The acoustic stimuli were broadcast with a calibrated custom-built ultrasonic electrostatic loudspeaker located contralateral to the recording site and at 60 cm from the bat's ear. A flat frequency response of the loudspeaker (± 1 dB) was obtained through digital filtering the playback stimuli with the inverse impulse response of the playback system as described in Luo and Moss (2017). Neural responses were recorded to 20 presentations of each stimulus. The order of stimulus presentation was randomized, and inter-stimulus set interval was 300 ms.

Electrophysiological recordings

Posts for head fixation during electrophysiological recordings were adhered to the skull with cyanoacrylate (Loctite 911), as described in Macías et al. (2018). Skull and brain surface landmarks were used to locate the IC and a ≤ 1 mm diameter craniotomy was made using a surgical drill. All neural recordings were carried out in a sound-attenuating and electrically-shielded chamber (Industrial Acoustics Company, Inc.). Bats were placed individually in a custom-made foam mold. The mold has a lid that restrains the bat's body movements and an elongated arm to which the head post is attached to maintain

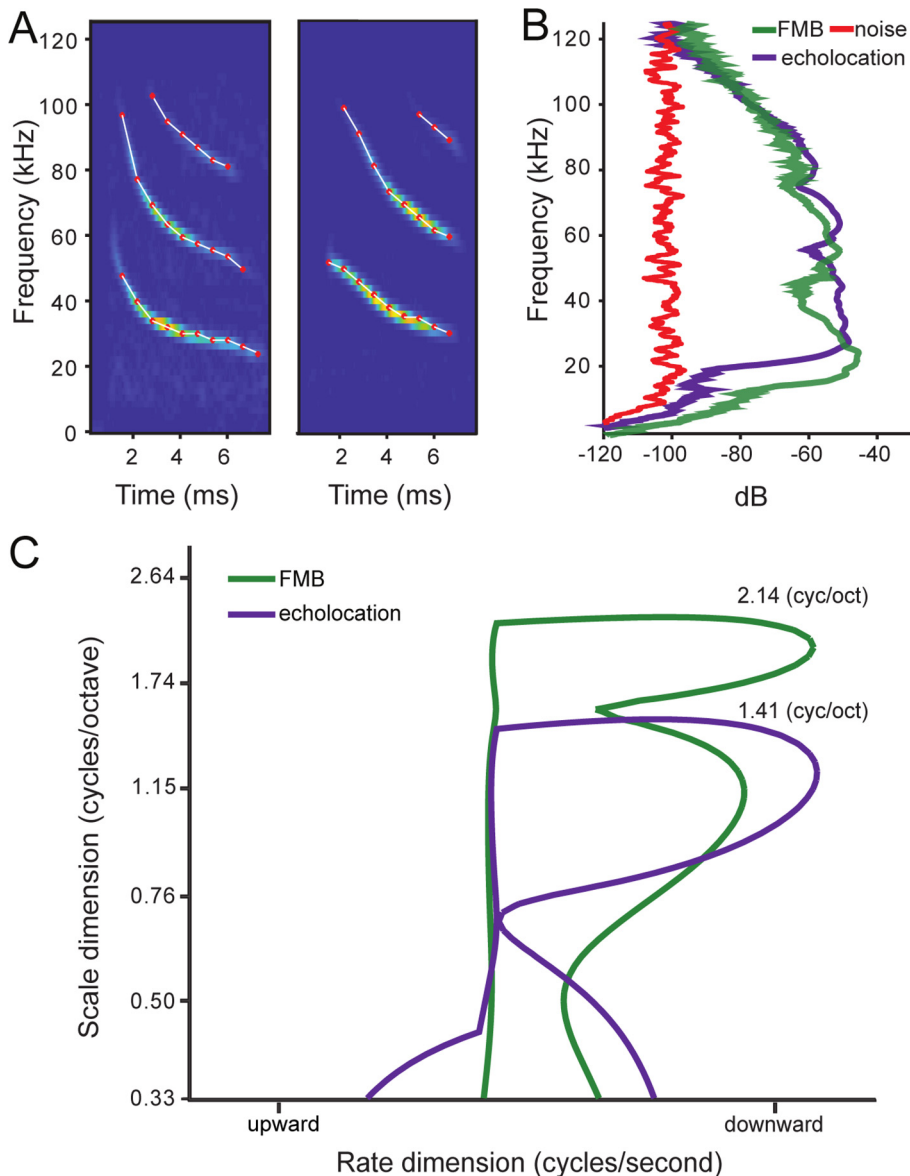


Fig. 1. Communication and echolocation calls overlap in spectral energy. **(A)** Spectrogram of example FMB element (left panel) and echolocation call (right panel) used as stimuli for the experiment. Data points and segments used for rate modulation analysis are marked in red and white lines respectively. **(B)** Power spectrum of isolated FMB and echolocation calls illustrate overlap in bandwidth of the two classes of signals. **(C)** SR plot showing the representation of FMB elements and echolocation calls on the rate (cycles/second) and scale (cycle/octave) dimensions.

the bat's head fixed during recordings. Recording sessions were carried out over 3–5 consecutive days for individual bats, each one lasting no more than 4 h. No drugs were administered during recordings.

A grounding electrode was a silver wire placed in between muscle and skull about 1 cm rostral to the craniotomy site. Neuronexus high impedance silicon probes were used for acute recordings (A1 × 16-5 mm-50-177-A16). A micromanipulator was used to situate the probe at the craniotomy site, orthogonally to brain surface. The probe's position at the surface of the brain was registered as 0 μm for depth reference. The shank was advanced in 10 μm steps using a hydraulic

microdrive (Stoelting Co.) mounted to the micromanipulator. Recording sites ranged in depth from 40 μm to 1620 μm . Neural responses were recorded at 16-bit precision and 40 kHz sampling rate using an OmniPlex D Neural Data Acquisition System recording system (Plexon, Inc.). A Transistor–transistor–logic (TTL) pulse for each stimulus presentation was generated with the National Instrument card described above and was recorded on one of the analog channels of the Plexon data acquisition system for synchronization of acoustic stimuli and neural recordings.

After electrophysiological recordings were completed, the site of the craniotomy was marked with a drop of India ink. Bats were then perfused with 4% PFA, brains were extracted and fixed further in 4% PFA for 24 h. Brains were transferred to 30% sucrose for 48 h and later sectioned in 50 μm slices using a cryostat (Leica CM1860). Nissl staining following the protocol described by the Cold Spring Harbor Laboratories (Paul et al., 2008) was used to verify electrode penetration sites in the IC (Fig. 2).

Analysis of neuronal recordings

Single units were detected and classified using 'Wave_clus', inspecting individual waveforms, as described in (Quiroga et al., 2004). Responses to stimuli were analyzed in windows of 25 ms duration, starting 5 ms after stimulus onset (99.9% of responses were found to have a latency above 5 ms from call onset). Units

with an average of less than five spike events over 20 stimulus presentations for both categories of stimuli were considered non-responsive and excluded from analysis. Multi-unit activity, determined from inter-spike intervals that were inconsistent with neuronal refractory periods (acceptance threshold for clusters: less than 10% of spikes with < 3 ms inter-spike interval) were excluded from analysis. The number of single units included in the data set reported here is 575. To visualize the responses to individual stimulus elements, raster plots were constructed using MATLAB and post-stimulus time histograms (PSTH, 2 ms bin width) were plotted. Number of spikes for each call within each response window was averaged across calls within a sequence and across sequences of the same category (FMB or echolocation).

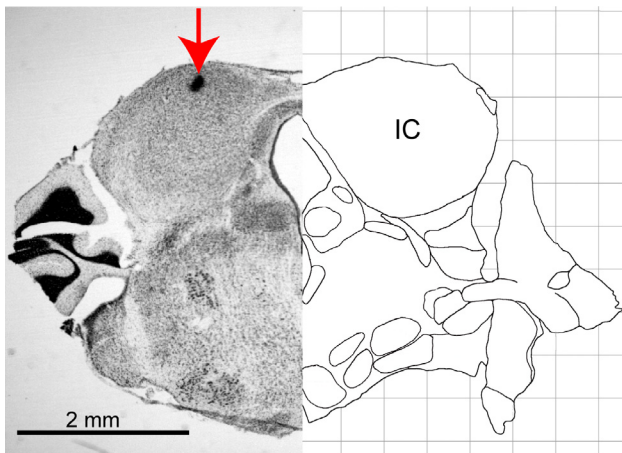


Fig. 2. Neural recording sites in the inferior colliculus of the big brown bat. The left half of the image is Nissl stain of a brain slice taken from one of the bats in this experiment. The right half of the image is Fig. 48 of the big brown bat atlas from the BatLab at the University of Washington (courtesy of Dr. E. Covey) for structural comparison. Red arrow indicates India ink mark made at electrode penetration site. (For interpretation of the references to colour in this figure legend, the reader is referred to the web version of this article.)

Frequency tuning curves, were constructed from the recordings taken in response to pure tones at different intensities described in the acoustic stimuli section. Best frequency at 70 dB SPL was calculated from spike number responses.

Spike triggered averages (STA), a 2D transfer function of the neuron, was estimated using the stimulus–response pairs under the linear system approximation of a neuron. A log-magnitude-spectrogram of the stimulus call, computed using a 1 ms window with 50% overlap, was used as the 2D stimulus for STA computation. A spike response was generated from the spike timings estimated using the ‘Wave_clus’ analysis. The STA was then computed using method described in Depireux and Elhilali (2013), by averaging 2D-stimulus snippets of duration 20 ms preceding a spike. STAs were derived separately from FMB and echolocation calls for each neuron and focused on comparing the characteristics of each of these functions. In addition to computing the mean of the stimulus snippets, we also computed the variance of every time–frequency point in the STA to highlight the spectro-temporal regions in the STA which have low variance and hence more reliable. Reliable regions of the STA were selected as time–frequency bins which have a variance lower than the 20% of the maximum variance in the STA. The reliable spectro-temporal regions of the STA are indicated in the figures as regions within black contours.

In order to validate the STA profiles, we quantified the prediction success of each type of STA (i.e. FMB and echolocation STA profiles). Prediction was performed based on the Linear Non-linear Poisson (LNP) cascade model (Chichilnisky, 2001; Schwartz et al., 2006). The LNP model consisted of three stages: (a) a linear stage that performs estimation of a strength of neural response to a stimulus using the following equation:

$$\hat{r}_i = \sum_{k=1}^K \sum_{l=1}^L H(t_k, f_l) S(t_k - t, f_l),$$

where \hat{r}_i is the response estimate for $H(t_k, f_l)$ which would be the STA and $S(t_k - t, f_l)$ which would be a given stimulus. Since a k would be used in an equation of probabilistic model, t_k indicates the k th time bin instead of k ; f_l is the l th frequency bin. (b) A non-linear stage that extracts intervals of activation candidates by applying a threshold to the strength estimate, and (c) a Poisson stage that determines how many spikes would occur within each interval. For each interval, the probability of the number of spikes was modeled as $P(k) = e^{-r\tau} (r\tau)^k / k!$ where k is a random variable that represents the number of spike, r is the occurrence rate, and τ the length of interval.

For assessment of prediction success, an additional stage for determining whether a candidate interval extracted in the non-linear stage is activated or not was performed based on Bernoulli trials whose event-probability can be represented as $P(\{\text{activated}\}) = \sum_{k=1}^{\infty} P(k) = 1 - P(k=0)$. As the result of Bernoulli trials on all candidates, activated intervals were finally obtained. If an activated interval included at least one spike, the activated interval would be defined as ‘Hit’, otherwise it was labeled a ‘False alarm’. A Receiver Operating Curve (ROC) was derived by noting the pairs, ‘Hit’ and ‘False alarm’ obtained for different thresholds applied in the non-linearity stage from 0.50 to 0.90 with 0.05 step. Note that ‘Hit rate’ and ‘False Alarm rate’ can be calculated by dividing the number of ‘Hit’ cases by the number of spikes and by dividing the number of ‘False Alarm’ cases by the time length for test, respectively.

In order to categorize neurons’ selectivity to FMB or FM echolocation stimuli, response characteristics based on spike rate and STA tuning were combined in six-dimensional feature vectors as follows: For each neuron, we noted the number of spikes for FMB and echolocation stimuli, as well as a ratio of the FMB to echolocation spike numbers. In addition, an F -score metric was derived from STA predictions to quantify prediction accuracy represented in ROC curves (Fig. 4C, D). F -score is defined as the harmonic mean of precision and recall where precision is calculated as the ratio of [hits] of [hits + false alarms], and recall is [hit rate] (Goutte and Gaussier, 2005). The maximum F -score derived from the STA–FMB prediction and STA–echolocation prediction (using FMB stimuli or echolocation stimuli, respectively), were extracted as additional 2D features. The ratio of F -scores, FMB–FMB over echolocation–echolocation, was considered as a last feature; resulting all together in a 6D feature vector for each neuron.

Next, a non-linear projection for each 6D feature vector from each neuron was performed using the ‘tSNE’ toolbox to map it from a high-dimensional manifold onto a 2D Euclidean space (van der Maaten and Hinton, 2008). This 2D space is then analyzed using Principal Component Analysis (PCA) where a k -mean clustering ($k = 3$) is performed to group the meaningful components into different classes (Strang, 2016). Clustering based on larger values of ($k = 4$) resulted in similar

grouping boundaries but further sub-divisions of clusters based on $k = 3$.

Statistical analysis

To quantify whether neurons responded selectively to FMB or echolocation signals, activity evoked by the two classes of stimuli were analyzed statistically, a Wilcoxon signed rank test was performed. To compare responses to FMB or echolocation stimuli, an FMB score was calculated as the ratio of the average responses to FMB's and echolocation calls. To measure whether male or female bats show differences in FMB- and echolocation-selective units, these ratios were pooled across animals and the two sex groups were compared using a Wilcoxon signed rank test. To determine whether there was a correspondence between the depth of a neuron in the IC and FMB-selectivity, a linear regression was performed between recording depth and the log of the FMB score, and the correlation coefficient and variance accounted for (R^2) were calculated. To assign neurons a categorical label from the spike number as FMB-preference or echolocation-preference, a permutation test was performed: The labels were removed from the raw data regarding whether a response was evoked by an FMB or echolocation stimulus. Then artificial labels were assigned to the raw data randomly, marking them as FMB or echolocation responses. This was repeated 100 times to generate a pool of randomized data. Then the analysis was repeated on those data and the FMB score calculated. 95% of the FMB scores fell in the interval of 0.740 and 1.352. Therefore, all units with an FMB or echolocation score outside that interval were considered as having FMB- or echolocation-preference units, with 95% confidence.

RESULTS

Echolocation and FMB's overlap in spectrotemporal features but retain distinctive characteristics

As noted above, FMB's and echolocation calls serve different behavioral functions in the big brown bat, yet they share spectral content. Each FMB is comprised of a sequence of three to four downward frequency modulated sweeps, as characterized by Wright and collaborators (Wright et al., 2014). Call interval of the signals in these natural bouts ranged from 21.22 ms to 28.4 ms. Duration of each of the calls in the bout averaged 6.3 ms, with a frequency bandwidth of 22–110 kHz over two harmonics. The FM echolocation sequences were constructed to match the pulse interval (PI) of calls in the FMB and used natural echolocation calls recorded from behaving bats (the PI ranged from 22.6 ms to 28.2 ms). Echolocation calls were approximately matched in duration to the FM bout elements ($5.9 \text{ ms} \pm 0.6 \text{ ms}$) and spanned a similar spectral bandwidth (27–110 kHz) (Fig. 1A). Even though the echolocation calls and FMB's show overlapping power spectra (Fig. 1B), they retain distinct temporal signatures that support functional categories. A close analysis of the FM of both sound groups shows a statistically significant difference in the FM slope

of the first harmonic (unpaired t -test, $t(df = 88) = 13.21$, $p < 0.005$). In addition, advanced signal processing analysis of FM profiles of 24 isolated calls for each category further confirms the separable characteristics of social and echolocation calls (Fig. 1C). These profiles show the spread of spectral modulations (cycles/octave) and temporal modulation rate (cycles/second) and reveal different distributions, with spread of spectral modulations of FMB's extending up to 2.14 cycles/octave and echolocation calls only up to 1.41 cycles/octave, and different profiles in the temporal dimension. These data suggest that social and echolocation calls, while largely overlapping in spectrum, retain spectro-temporal signature characteristics that could convey different information.

FMB's and echolocation sequences elicit different responses in single units in the IC

We analyzed single unit responses in the IC of the awake big brown bat to FMB's and echolocation call sequences (Fig. 3A). To control for the influence of call duration on the neural responses, we constructed the echolocation sequences with four calls matched in duration to the FMB elements ($5.9 \pm 0.6 \text{ ms}$). For some units, the FMB social calls elicited consistent firing across the four calls within the bout and across the six different exemplars of the category, while showing low firing rates to a sequence of echolocation calls presented at the same interval as the natural FMB (PIs ranged from 22.6 ms to 28.2 ms) (Fig. 3Bi). On the other hand, some units showed weak responses to the FMB's but consistent firing to the echolocation call sequences (Fig. 3Bii). We averaged the responses to each call within a sequence and then calculated the mean response across exemplars. Responses to echolocation sequences and FMB's were significantly different across the population of units (Wilcoxon signed rank test, $Z = 11.23$, $p < 0.0001$). We performed a permutation test for the random distribution of the responses to FMB's and echolocation calls and established limits at 95% confidence intervals using 100 iterations (Fig. 3C). Of the 575 analyzed single units, 34% showed spike number responses for FMB/echolocation ratio above the permutation test limit, (units responding preferentially to FMB stimuli), while 10% showed spike number responses for the FMB/echolocation ratio below permutation test limit (units that respond preferentially to echolocation stimuli), and 56% fell between the permutation test limits, indicating no selectivity (Fig. 3D). False positives predicted by the permutation test would occur at most in 2.5% of either category. Thus, there are populations of neurons in the IC of big brown bats that respond differentially to FM echolocation and FMB communication calls with overlapping spectra and matching sound duration.

STA analysis reveals sub-populations of neurons whose selectivity is also driven by precise response timing

We probed the spectro-temporal stimulus information evoking responses in different populations of neurons in the IC using STA analysis, and derived a unit's tuning

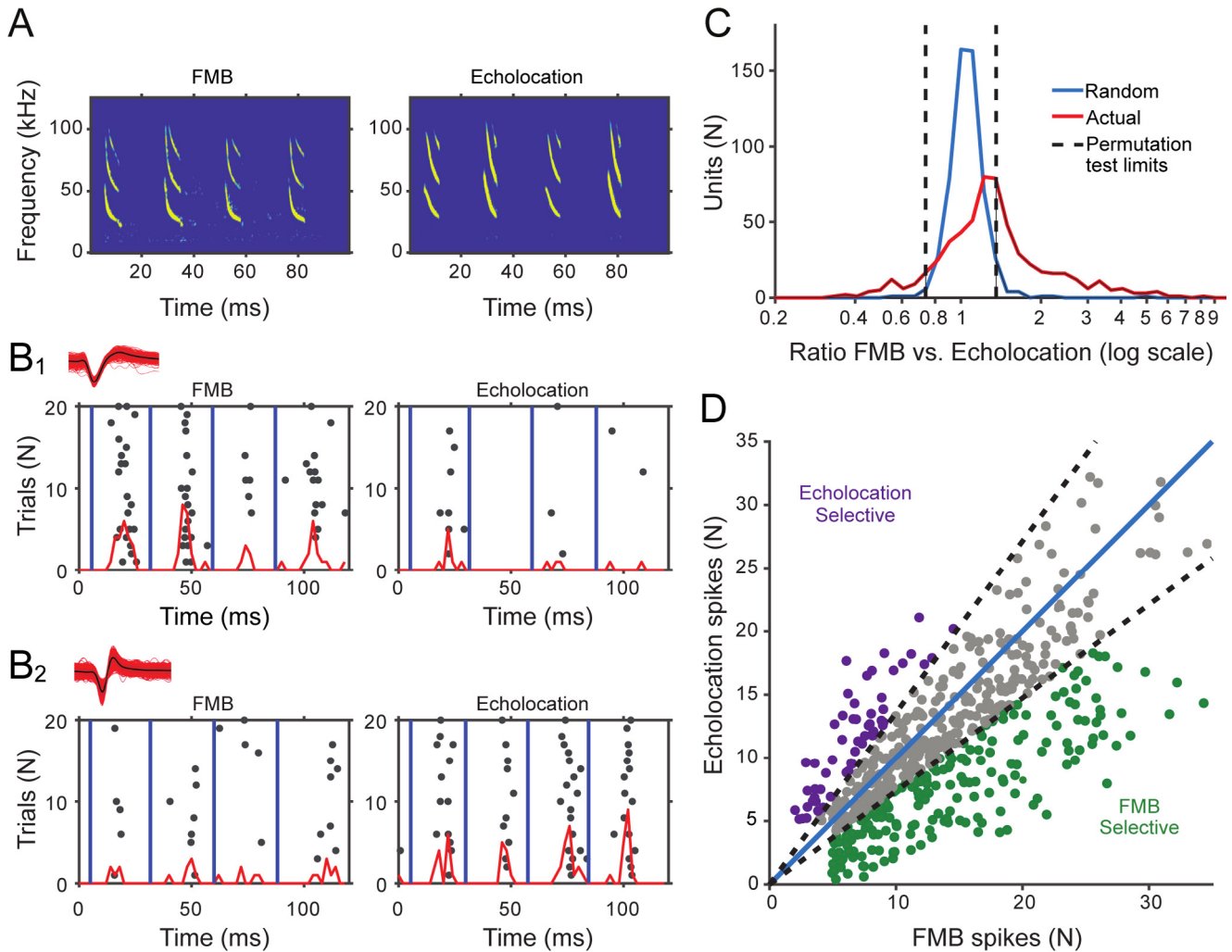


Fig. 3. Selective responses in the inferior colliculus of the big brown bat revealed by spike number. **(A)** Spectrograms showing examples of the FMB (left panel) and echolocation (right panel) stimuli used for the experiment. **(B)** Raster plots and PSTH (red) of example unit responses to 20 presentations of an FMB or an echolocation sequence for **(B1)** an FMB selective unit and **(B2)** an echolocation selective unit. Insets show waveforms obtained by spike sorting. Grey dots indicate spike events for each trial. Vertical blue lines indicate call onset. Red line indicates PSTH with a 2 ms bin size. **(C)** Distribution of units respect to response ratio is shown for the permutation test random distribution (blue line) and the actual distribution of units (red line). Black dashed vertical lines indicate 95% lower limit (left) and upper limit (right) for the permutation test. Shaded area shows units that fall outside the permutation limits. **(D)** Scatter plot shows single unit mean spike number for FMBs (x axis) and echolocation calls (y axis). Each circle in the graph represents a different unit. Dotted black lines mark the permutation test 95% limit for random distribution. Gray circles indicate units that show no selectivity, green circles indicate units with FMB selectivity and purple circles indicate echolocation selectivity. Blue line indicates equal response for both categories. (For interpretation of the references to colour in this figure legend, the reader is referred to the web version of this article.)

profile in response to either FMB or echolocation calls. STA responses varied across neurons, with many units showing clear STA's either to FMB's or echolocation calls, but not both. Fig. 4A shows an example unit of an FM-selective STA with clear tuning to spectrotemporal patterns of FMB stimuli but not echolocation calls; while Fig. 4B shows another unit with clear tuning selectivity to echolocation but not FMB stimuli. We validated the STA analysis by calculating the prediction efficiency to held-out stimuli for each category. For example, at a fixed false alarm rate of 0.25 (a trade-off point where the false alarm rate is low but we still have good detection rates) FMB-selective STA's correctly predict 65.44% of the responses to FMB stimuli while they only predict 45.61% of the responses to echolocation stimuli (Fig. 4C). On the other hand, echolocation-selective

STA's correctly predict 44.98% of the responses to echolocation stimuli but only 17.65% of the correct responses to FMB's at the same false alarm rate condition (Fig. 4D). These results indicate that spectrotemporal stimulus features are key to the discrimination of echolocation and communication calls by single neurons in the bat IC.

We also compared findings obtained from two different classification methods, the ratio of FMB over echolocation for the spike number and the ratio for the FMB over echolocation for F-scores obtained from the STA validation. This analysis revealed a high correlation between the two classification methods, with a coefficient of 0.6973, $p < 0.0001$ (Fig. 5). Furthermore, 59% of the units classified as echolocation-selective by the spike count criterion were also similarly classified by

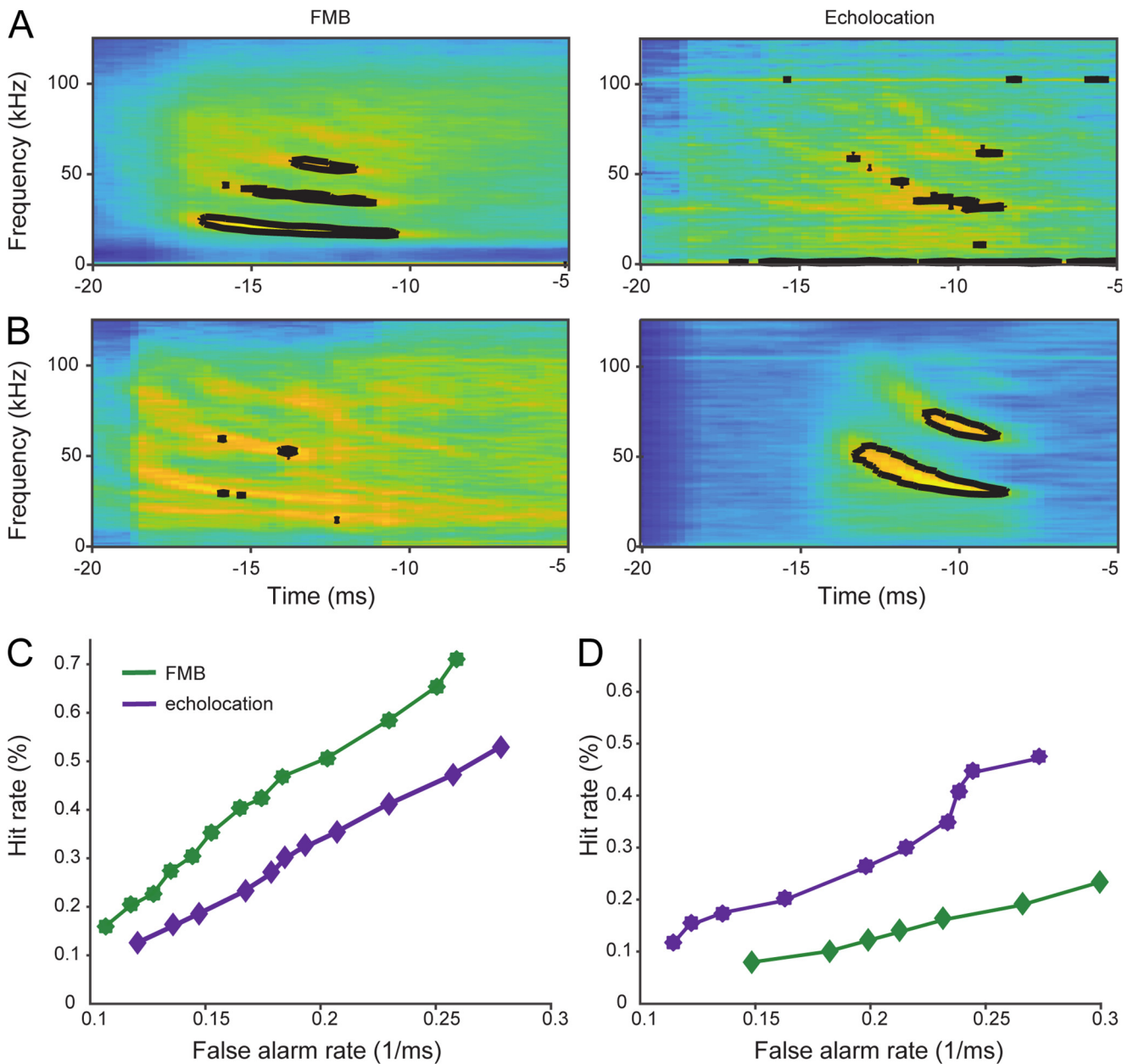


Fig. 4. Examples of spike-triggered average analysis (STA), assuming linear transfer functions for each category of stimulus. FMB (upper panel) or echolocation (lower panel). Example of normalized STA for the echolocation and FMB stimuli for (A) a unit that shows FMB selectivity and for (B) a unit showing echolocation selectivity in both strength and timing of response. Black contours denote reliable areas of the STRF with variance lower than 20% of the maximum variance. (C) Prediction of responses to FMB and echolocation using the calculated echolocation STA. (D) Prediction of responses to FMB and echolocation using the calculated FMB STA.

the STA's. In this way, two sub-populations of neurons emerge, where selectivity was not only dependent on the strength of response but also by the precise timing of responses to FMB or FM echolocation stimuli, as inferred using the STA's.

Combination of spike number analysis and STA response prediction test reveals clusters of FMB or echolocation selective units

We probed the selectivity of IC neurons of big brown bats by jointly analyzing their spike number and STA

responses to communication or echolocation calls. A combination of six features was extracted from each unit's response to reflect both its spike rate and STA; the combination of features was projected onto a lower dimensional space along the most informative component (see methods). A clustering of this mapping revealed three clusters of units (Fig. 6, Table 1). The first cluster is comprised of FMB-selective units that show higher spike number for the FMB stimuli than for the echolocation stimuli and a higher STA prediction score for FMB than echolocation calls (green in Fig. 6B and Table 1). The second cluster is comprised of

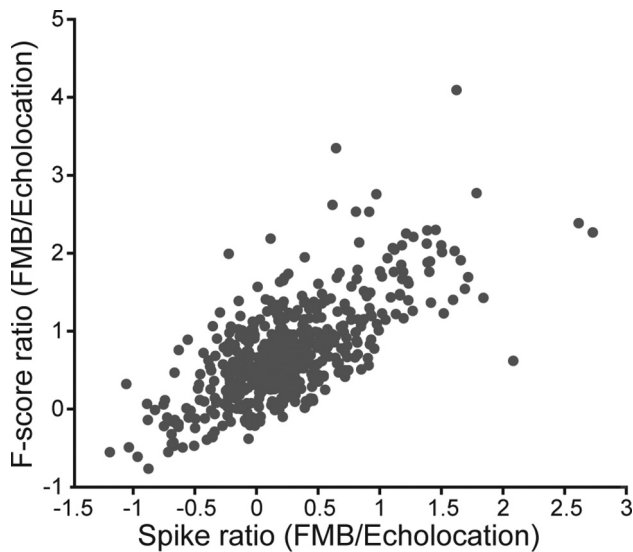


Fig. 5. Correlation between ratios of FMB: echolocation spike number and FMB: echolocation STA *F*-score. All units are shown (red dots) for their spike number ratio (FMB/echolocation) on the x-axis and for their *F*-score ratio (FMB/Echolocation) on the y-axis obtained from the STA. The correlation coefficient is 0.6973.

echolocation-selective units that have higher spike number for echolocation than for the FMB stimuli, and show a higher STA prediction score for echolocation than FMB signals (purple in Fig. 6B and Table 1). The third cluster contains non-selective units that show small differences and contradictory spike numbers (higher for FMB stimuli) and scores (higher for echolocation stimuli) (gray in Fig. 6B and Table 1). This analysis shows a robust classification of units in the IC of the big brown bat that either preferentially respond to the FMB stimuli or to the echolocation stimuli, or show no selectivity to either sound category.

Differentially responsive units occur in both males and females

As noted above, FMB's are hypothesized to serve a food-claiming function in big brown bats, because they predict foraging success of the individual producing these social calls. Although these calls are only emitted by male big brown bats, behavioral studies show that they serve the same function in male and female conspecific listeners: Previous research on competitive foraging in big brown bats showed that inter-bat distance increased after an animal emitted an FMB sequence, both when the listening bat was male and when it was female (Wright et al., 2014). The finding that both sexes increase inter-bat distance after FMB emissions led us to investigate if the representation of the FMB-selective neural populations in both males and females. Of the five bats used in this study, two were male and three were female. We found that FMB-selective and echolocation-selective units occur in both male and female bats, with no significant difference in their representation between sexes for spike number selectivity ratio (Wilcoxon signed rank test, $Z = -0.6359$, $p = 0.52$; Fig. 7A), and for the combined spike number and STA validation (Wilcoxon signed rank

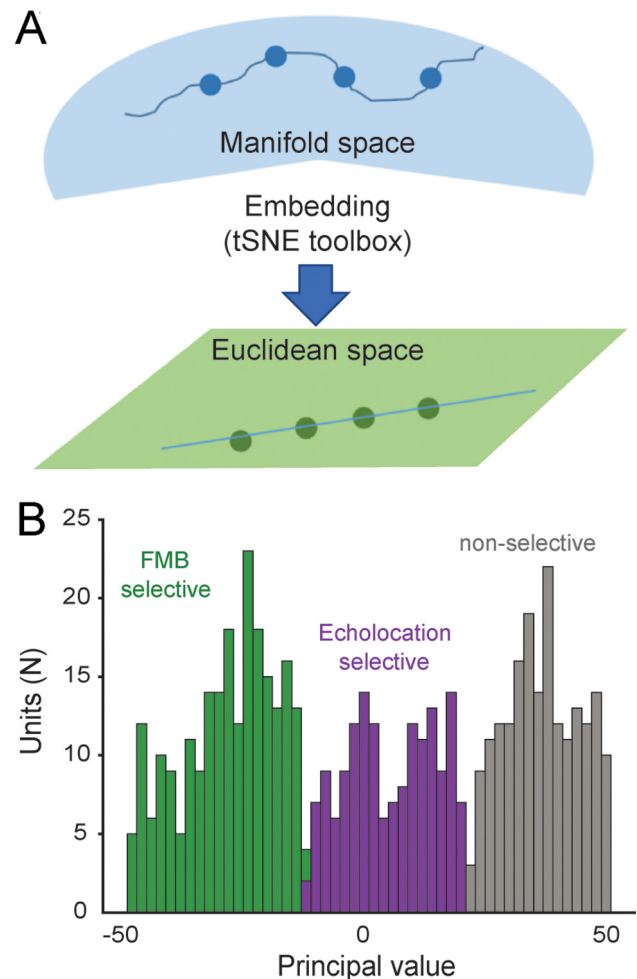


Fig. 6. Combination of spike number analysis and STA reveals clusters of FMB or echolocation selective units. (A) Diagram representing the method by which each unit containing 6D embedded features to be represented in a 2D space. (B) Distribution along the PCA revealing three separate clusters, an FMB selective cluster, an echolocation selective cluster and a non-selective cluster (see Table 1 for details).

test; FMB selective cluster $Z = -1.2222$, $p = 0.22$; Echolocation selective cluster $Z = 1.4529$, $p = 0.14$; Fig. 7B).

FMB and echolocation call selective units are present along the dorsal–ventral axis of the bat IC

There is a wealth of data reporting that the IC of the big brown bat is tonotopically organized (Covey, 2005; Poon et al., 1990). This was corroborated in our recordings: neurons in the dorsal IC were tuned to lower sound frequencies, and neurons in the ventral IC were tuned to higher sound frequencies ($R^2 = 0.455$; Fig. 8A). Even though the echolocation calls and FMB's show overlapping power spectra (Fig. 1B), there is a range of lower frequencies of the calls (22–27 kHz) where the FMB elements have ~20 dB more energy. If the FMB response selectivity were only due to the response of a population of neurons tuned to lower frequencies, this difference in spectral energy among the calls would bias the FMB

Table 1. Results from the combined spike number and STA score reveals three clusters of units

Mean std.	FMB selective cluster	Echolocation selective cluster	All neurons	Non-selective cluster
Spike R (F/E)	1.3247	0.6302	1.00	0.9218
FMB spikes	0.6966	0.7624	1.00	1.5556
Echolocation spikes	0.5530	1.0406	1.00	1.4954
Score R (F/E)	1.5274	0.5186	1.00	0.7741
F-F score	0.7637	0.8658	1.00	1.3906
E-E score	0.4957	1.2422	1.00	1.3964

The FMB selective cluster of units is characterized by a higher ratio of number of spikes for the FMB stimuli than for the echolocation stimuli, and by a higher ratio of the FMB score in the STA than for echolocation (green column, red boxes). The echolocation selective cluster is characterized by a higher ratio of number of spikes for the echolocation stimuli than for the FMB, and a higher ratio of the echolocation score from the STA (purple column, red boxes). The cluster of non-selective units is characterized by having small and contradictory differences in both spike number ratio (higher for FMB) and STA scoring (higher for echolocation) (gray column, red boxes).

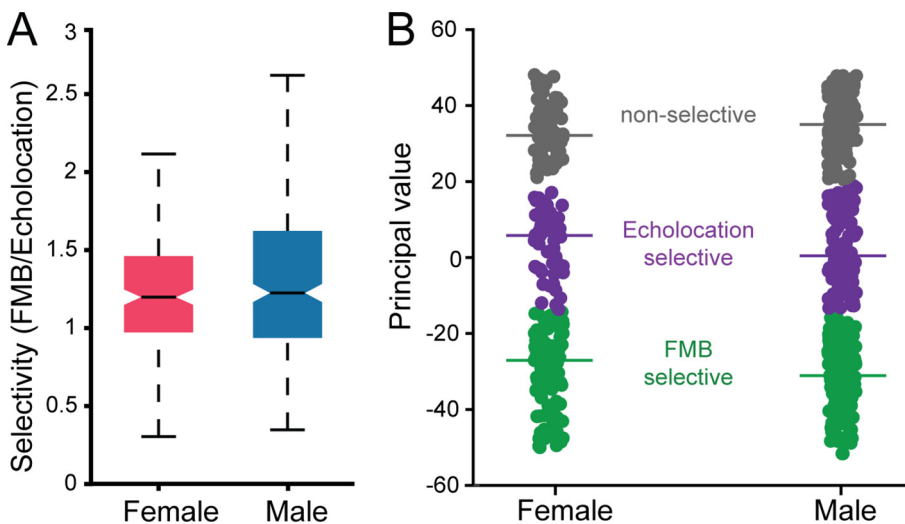


Fig. 7. Stimulus selectivity is present in both males and females. **(A)** Selectivity ratio (calculated as mean spike number for FMB/mean spike number for echolocation) for all units from female and male bats. **(B)** Unit distribution for females and males according to the classification clusters. Each circle in the graph represents a different unit. Green circles are units belonging to the FMB-selective cluster, purple circles are units belonging to the echolocation-selective cluster and gray circles are units belonging to the non-selective cluster. (For interpretation of the references to colour in this figure legend, the reader is referred to the web version of this article.)

selective units to be found at more dorsal locations of the IC, where neurons tend to show tuning to lower sound frequencies. We mapped the depth distribution of FMB-selective and echolocation-selective neurons in the bat IC. This analysis showed that FMB-selective units and echolocation-selective units occur throughout the dorsal–ventral axis of the IC, showing no systematic trend for FMB-selective units in more dorsal regions (Linear fit: slope = 2.1 ± 3.7) (Fig. 8B). Thus, it is reasonable to think that FMB selective neurons have broader and/or more complex receptive fields. Indeed, only 3% of the variance for selectivity on the combined spike number and STA validation can be explained by recoding depth ($R^2 = 0.03$). These results, taken together with the STA's, show that fine spectro-temporal features of echolocation and FMB stimuli give rise to neural call selectivity.

DISCUSSION

Neural mechanisms for natural stimulus processing have been identified in birds, mice and bats, revealing specializations to detect and discriminate behaviorally relevant acoustic signals. Here we provide the first demonstration of neural selectivity to functionally characterized social signals in the bat midbrain and show that this stimulus selectivity depends on the temporal fine structure of natural sounds.

In both avian and mammalian systems, a strong relationship between tuning of midbrain neurons and the spectrotemporal features of conspecific vocalizations has been described (reviewed in Woolley and Portfors (2013)). Temporal processing of acoustic signals contributes directly to animal communication (Suta et al., 2008; Schneider and

Woolley, 2010; reviewed in Helekar (2013); Comins and Genter, 2014); it has been shown that small acoustic differences in temporal features can translate to large perceptual differences (Pisoni, 1977; Kuhl and Miller, 1978; Burns and Ward, 1978; Kuhl 1981; Kuhl, 1983). In our study, advanced signal processing methods revealed fine differences in the temporal structure of call categories of the frequency modulated signals that bats use for echolocation and social communication. This motivates the hypothesis that acoustic temporal structure of natural sounds serves to guide action-selection decisions in freely-behaving bats.

For bats, the role of the IC in echolocation call processing has been studied in detail (Reviewed in Wenstrup and Portfors (2011)), but far less is known about the function of this midbrain structure in the processing of communication calls. Communication call

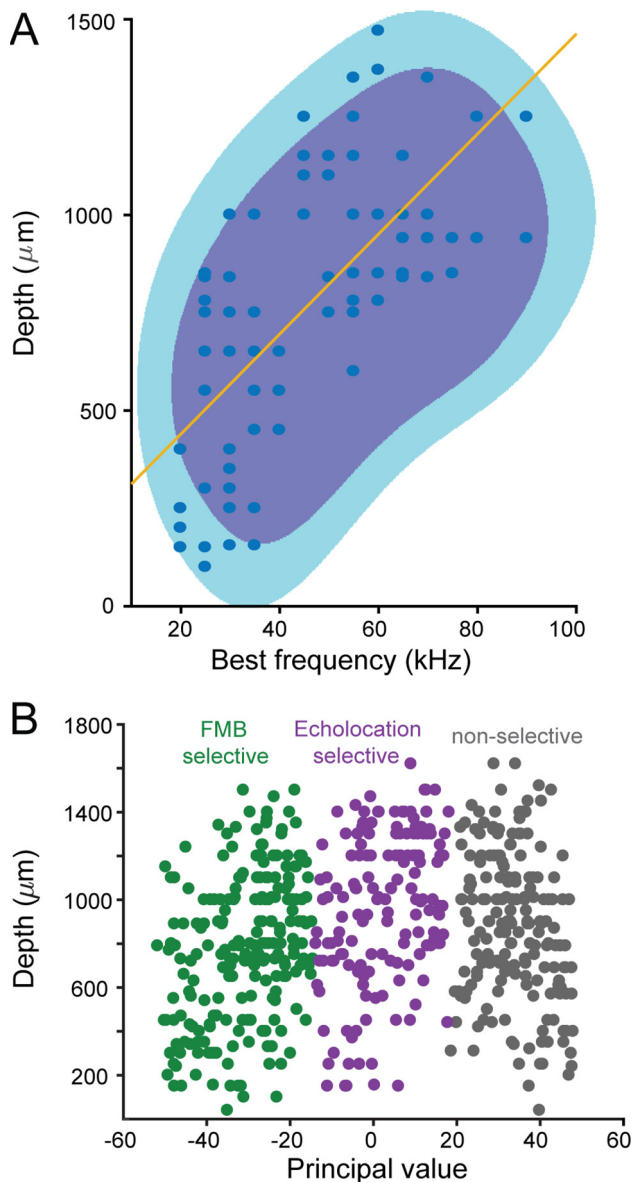


Fig. 8. Selectivity to FMB and echolocation signals is distributed throughout the tonotopically organized IC. (A) Best frequency (BF) of single neurons measured at 70 dB SPL as a function of recording depth. Orange line shows linear fit to the data. Purple and aqua areas represent Gaussian filtered heat-map of best frequency by depth data. (B) Distribution of selectivity classification across the dorsal-ventral axis of the IC. Each circle in the graph represent a different unit. Green circles are units belonging to the FMB-selective cluster, purple circles are units belonging to the echolocation-selective cluster and gray circles are units belonging to the non-selective cluster. (For interpretation of the references to colour in this figure legend, the reader is referred to the web version of this article.)

selectivity in the IC has so far been described in only two species of bats, the Mexican free-tailed bat and the mustached bat (reviewed in Pollak (2011)). As shown in mice, inhibitory pathways modulate complex call selectivity in the Mexican free-tailed bat (Klug et al., 2002). Importantly, previous studies in bats have not explored neural selectivity to functionally characterized social calls that share spectral features with echolocation calls. Here, we bridge this gap by demonstrating neural selectivity of sin-

gle IC neurons to natural FMB's that show overlap in spectral power with echolocation calls, but carry different behavioral information.

Neurophysiological recordings in the Mexican free-tailed bat and the mustached bat show that response selectivity to pure tones did not predict response selectivity to complex calls (Andoni and Pollak, 2011; Brimijoin and O'Neill, 2005; Holmstrom et al., 2007; Portfors, 2004). Our results are consistent with these earlier reports and, also show that FMB-selective and echolocation-selective neurons are distributed throughout the dorso-ventral tonotopic axis of the IC of the big brown bat. Our data indicates that natural sound selectivity in the IC of this species is tied to the time-frequency structure of its calls.

Several studies suggest the importance of stimulus duration in call selectivity in bats (Casseday et al., 1994; Ehrlich et al., 1997; Jen et al., 2012). To control for sound duration in our study, we compared neural responses to echolocation calls matched in duration to the FMB elements. Our data show that call duration does not drive call selectivity in FMB-selective units, but instead FM sweep rate is a key variable. A recent study in the big brown bat reported neurons in the IC tuned to specific sweep rates (Morrison et al., 2018), and even though this study did not directly investigate communication call selectivity, the findings are consistent with the data reported here. Specifically, our results show that signal sweep rate contributes to selectivity of IC neurons to natural calls that have different behavioral functions.

In the mustached bat, spectro-temporal receptive field analysis of IC neurons revealed that responses depend on the time-frequency structure of the stimulus (Brimijoin and O'Neill, 2010). With this evidence, Brimijoin & O'Neill propose that the IC serves as a pattern detector, in which neurons respond selectively to call features. In our study, we computed spike-triggered averages (STA's) for each stimulus category, which revealed distinct subpopulations of neurons selective to echolocation or FMB stimuli. We then combined the information obtained from the spike number and the STA revealing clusters of neurons selective for FMB or echolocation calls, both in the strength and timing of their responses. This raises the possibility that neurons might convey stimulus information through temporal response characteristics, thus contributing to the behavioral discrimination of calls.

Many species of bats use social calls to communicate relevant information in different behavioral contexts, such as mate attraction, pup isolation and aggression, but it is not always both sexes that emit or respond to a specific call (reviewed in Chaverri et al. (2018)). For example, only male big brown bats produce the FMB, but both sexes show behavioral responses to FMB's (Wright et al., 2014). Thus, we characterized FMB call-selective neurons in both sexes. We found that differential selectivity to echolocation and FMB calls is present in comparable proportions in both males and females, consistent with the behavioral data reported by Wright et al. (2013).

In summary, we report here single unit data demonstrating that the features of social and echolocation signals of the big brown bat activate

separate populations of neurons in the IC, and this neural selectivity could enable rapid parsing of acoustic signals that carry different semantic content. Further, we show that neither stimulus spectrum nor duration alone can account for the selectivity of single IC neurons, but instead is tied to differences in the fine spectro-temporal structure of calls used for echolocation and social communication. Future experiments that directly investigate circuit dynamics of IC neurons can uncover specific mechanisms that give rise to stimulus selectivity in bats and other animals that must analyze complex auditory scenes to guide survival behaviors in the natural environment.

CONFLICT OF INTERESTS

The authors declare no competing financial interests.

ACKNOWLEDGEMENTS

We thank Dr. Jinhong Luo for LabView code for stimulus playback, Dr. Michaela Warnecke and Dr. Chen Chiu for sharing audio data and Bruce Nguyen Tran for help during data pre-processing. This work was funded by Human Frontiers Science Program fellowship awarded to AS (LT000220/2018), Brain Initiative (NSF-FO 1734744 (2017–2021), AFOSR (FA9550-14-1-0398NIFTI) and ONR (N00014-17-1-2736).

REFERENCES

- Andoni S, Pollak GD (2011) Selectivity for spectral motion as a neural computation for encoding natural communication signals in bat inferior colliculus. *J Neurosci* 31:16529–16540. <https://doi.org/10.1523/JNEUROSCI.1306-11.2011>.
- Brimijoin WO, O'Neill WE (2010) Patterned tone sequences reveal non-linear interactions in auditory spectrotemporal receptive fields in the inferior colliculus. *Hear Res* 267:96–110. <https://doi.org/10.1016/j.heares.2010.04.005>.
- Brimijoin WO, O'Neill WE (2005) On the prediction of sweep rate and directional selectivity for FM sounds from two-tone interactions in the inferior colliculus. *Hear Res* 210:63–79. <https://doi.org/10.1016/j.heares.2005.07.005>.
- Burns EM, Ward WD (1978) Categorical perception – phenomenon or epiphenomenon: evidence from experiments in the perception of melodic musical intervals. *J Acous Soc Am* 63:456. <https://doi.org/10.1121/1.381737>.
- Casseday JH, Ehrlich D, Covey E (1994) Neural tuning for sound duration: role of inhibitory mechanisms in the inferior colliculus. *Science* 264:847–850.
- Chaverri G, Ancillotto L, Russo D (2018) Social communication in bats. *Biol Rev* 93:1938–1954. <https://doi.org/10.1111/brv.12427>.
- Cherry EC (1953) Some Experiments on the recognition of speech, with one and with two ears. *J Acous Soc Am* 25:975–979. <https://doi.org/10.1121/1.1907229>.
- Chi T, Ru P, Shamma SA (2005) Multiresolution spectrotemporal analysis of complex sounds. *J Acoust Soc Am* 118:887–906.
- Chichilnisky EJ (2001) A simple white noise analysis of neuronal light responses. *Network* 12:199–213. <https://doi.org/10.1080/net.12.2.199.213>.
- Chiu C, Xian W, Moss CF (2008) Flying in silence: Echolocating bats cease vocalizing to avoid sonar jamming. *PNAS* 105:13116–13121. <https://doi.org/10.1073/pnas.0804408105>.
- Comins JA, Genter TQ (2014) Temporal patter processing in songbirds. *Curr Opin Neurobiol* 28:179–187. <https://doi.org/10.1016/j.conb.2014.08.003>. Epub 2014 Sep 15.
- Covey E (2005) Neurobiological specializations in echolocating bats. *Anat Rec A Discov Mol Cell Evol Biol* 287:1103–1116. <https://doi.org/10.1002/ar.a.20254>.
- Depireux DA, Elhilali M (2013) *Handbook of modern techniques in auditory cortex*. Nova Science Publishers.
- Ehrlich D, Casseday JH, Covey E (1997) Neural tuning to sound duration in the inferior colliculus of the big brown bat, *Eptesicus fuscus*. *J Neurophysiol* 77:2360–2372. <https://doi.org/10.1152/jn.1997.77.5.2360>.
- Goutte C, Gaussier E (2005) A probabilistic interpretation of precision, recall and F-score, with implication for evaluation. In: Losada DE, Fernández-Luna JM, editors. *Advances in information retrieval, lecture notes in computer science*. Berlin Heidelberg: Springer. p. 345–359.
- Griffin DR (1958) *Listening in the dark: the acoustic orientation of bats and men, listening in the dark: the acoustic orientation of bats and men*. Oxford, England: Yale Univer. Press.
- Helekar SA, editor. *Animal models of speech and language disorders*. New York: Springer-Verlag.
- Holmstrom L, Roberts PD, Portfors CV (2007) Responses to social vocalizations in the inferior colliculus of the mustached bat are influenced by secondary tuning curves. *J Neurophysiol* 98:3461–3472. <https://doi.org/10.1152/jn.00638.2007>.
- Jen PH-S, Wu CH, Wang X (2012) Dynamic temporal signal processing in the inferior colliculus of echolocating bats. *Front Neural Circuits* 6:27. <https://doi.org/10.3389/fncir.2012.00027>.
- Klug A, Bauer EE, Hanson JT, Hurley L, Meitzen J, Pollak GD (2002) Response selectivity for species-specific calls in the inferior colliculus of Mexican free-tailed bats is generated by inhibition. *J Neurophysiol* 88:1941–1954. <https://doi.org/10.1152/jn.2002.88.4.1941>.
- Kuhl PK, Miller JD (1978) Speech perception by the chinchilla: identification function for synthetic VOT stimuli. *J Acoust Soc Am* 63(3):905–917. <https://doi.org/10.1121/1.381770>.
- Kuhl PK (1981) Discrimination of speech by nonhuman animals: Basic auditory sensitivities conducive to the perception of speech sound categories. *J Acoust Soc Am* 70:340. <https://doi.org/10.1121/1.386782>.
- Kuhl PK (1983) Enhanced discriminability at the phonetic boundaries for the place feature in macaques. *J Acoust Soc Am* 73:1003. <https://doi.org/10.1121/1.389148>.
- Lewicki MS, Olshausen BA, Surtlykke A, Moss CF (2014) Scene analysis in the natural environment. *Front Psychol* 5. <https://doi.org/10.3389/fpsyg.2014.00199>.
- Luo J, Moss CF (2017) Echolocating bats rely on audiovocal feedback to adapt sonar signal design. *PNAS* 114:10978–10983. <https://doi.org/10.1073/pnas.1711892114>.
- van der Maaten L, Hinton G (2008) Visualizing data using t-SNE. *J Mach Learn Res* 9:2579–2605.
- Macías S, Luo J, Moss CF (2018) Natural echolocation sequences evoke echo-delay selectivity in the auditory midbrain of the FM bat, *Eptesicus fuscus*. *J Neurophysiol* 120:1323–1339. <https://doi.org/10.1152/jn.00160.2018>.
- Morrison JA, Valdizón-Rodríguez R, Goldreich D, Faure PA (2018) Tuning for rate and duration of frequency-modulated sweeps in the mammalian inferior colliculus. *J Neurophysiol* 120:985–997. <https://doi.org/10.1152/jn.00065.2018>.
- Paul CA, Beltz B, Berger-Sweeney J (2008) The Nissl stain: a stain for cell bodies in brain sections. *Cold Spring Harb Protoc*. <https://doi.org/10.1101/pdb.prot4805>. <https://doi.org/10.1101/pdb.prot4805>.
- Pollak GD (2011) Discriminating among complex signals: the roles of inhibition for creating response selectivities. *J Comp Physiol A Neuroethol Sens Neural Behav Physiol* 197:625–640. <https://doi.org/10.1007/s00359-010-0602-9>.
- Poon PW, Sun X, Kamada T, Jen PH (1990) Frequency and space representation in the inferior colliculus of the FM bat, *Eptesicus fuscus*. *Exp Brain Res* 79:83–91.
- Popper AN, Fay RR (1995) *Hearing by bats*, Springer handbook of auditory research. New York, NY: Springer-Verlag.
- Portfors CV (2004) Combination sensitivity and processing of communication calls in the inferior colliculus of the Mustached

- Bat *Pteronotus parnellii*. *An Acad Bras Cienc* 76:253–257. <https://doi.org/S0001-37652004000200010>.
- Quiroga RQ, Nadasdy Z, Ben-Shaul Y (2004) Unsupervised spike detection and sorting with wavelets and superparamagnetic clustering. *Neural Comput* 16:1661–1687. <https://doi.org/10.1162/089976604774201631>.
- Sayegh R, Aubie B, Faure PA (2011) Duration tuning in the auditory midbrain of echolocating and non-echolocating vertebrates. *J Comp Physiol A Neuroethol Sens Neural Behav Physiol* 197:571–583. <https://doi.org/10.1007/s00359-011-0627-8>.
- Schneider DM, Woolley SMN (2010) Discrimination of communication vocalizations by single neurons and groups of neurons in the auditory midbrain. *J Neurophysiol* 103:3248–3265. <https://doi.org/10.1152/in.01131.2009>.
- Schnitzler H-U, Kalko EKV (2001) Echolocation by Insect-Eating Bats We define four distinct functional groups of bats and find differences in signal structure that correlate with the typical echolocation tasks faced by each group. *Bioscience* 51:557–569. [https://doi.org/10.1641/0006-3568\(2001\)051\[0557:EBIEB\]2.0.CO;2](https://doi.org/10.1641/0006-3568(2001)051[0557:EBIEB]2.0.CO;2).
- Schwartz O, Pillow JW, Rust NC, Simoncelli EP (2006) Spike-triggered neural characterization. *J Vis* 6:484–507. <https://doi.org/10.1167/6.4.13>.
- Strang Gilbert (2016) Chapter 7.3 Principal component analysis. Introduction to linear algebra. Wellesley-Cambridge Press.
- Suta D, Popelár J, Syka J (2008) Coding of communication calls in the subcortical and cortical structures of the auditory system. *Physiol Res* 57(Suppl 3):S149–S159.
- Thomas J, Vater M, Moss CF (2003) Echolocation in bats and dolphins.
- Wenstrup JJ, Portfors CV (2011) Neural processing of target distance by echolocating bats: functional roles of the auditory midbrain. *Neurosci Biobehav Rev* 35:2073–2083. <https://doi.org/10.1016/j.neubiorev.2010.12.015>.
- Woolley SMN, Portfors CV (2013) Conserved mechanisms of vocalization coding in mammalian and songbird auditory midbrain. *Hear Res* 305:45–56. <https://doi.org/10.1016/j.heares.2013.05.005>.
- Wright GS, Chiu C, Xian W, Moss CF, Wilkinson GS (2013) Social calls of flying big brown bats (*Eptesicus fuscus*). *Front Physiol* 4. <https://doi.org/10.3389/fphys.2013.00214>.
- Wright GS, Chiu C, Xian W, Wilkinson GS, Moss CF (2014) Social calls predict foraging success in big brown bats. *Curr Biol* 24:885–889. <https://doi.org/10.1016/j.cub.2014.02.058>.

(Received 5 August 2019, Accepted 28 November 2019)
(Available online 7 January 2020)